Plate impact shock experiments and numerical modeling of lightweight adobe masonry material

Christoph Sauer[1,*], *Frank* Bagusat[1], *Andreas* Heine[1], and *Werner* Riedel[1]

[1]Fraunhofer Institute for High-Speed Dynamics, Ernst-Mach-Institut, EMI, Eckerstr. 4, 79104 Freiburg, Germany

Abstract. In this contribution, we summarize and extend the experimental and numerical investigation of the shock response of lightweight adobe masonry, previously published in [C. Sauer et al., J. Dyn. Behav. Mater. (submitted)]. It is demonstrated that inverse planar plate impact (PPI) experiments are feasible for lightweight adobe. From the obtained free surface velocity time curves, a linear shock velocity vs. particle velocity relation is derived within the measured range of particle velocities. Numerical simulations of these curves show that the employed homogenous numerical model is capable of properly treating the shock response of this porous, inhomogeneous, and low-strength material. This numerical model is then applied to the example of the ballistic impact of steel spheres on targets consisting of one lightweight adobe brick. The experimentally obtained penetration craters are properly reproduced by the simulated target damage. Moreover, we find good agreement of the measured and simulated residual velocities within the presented range of impact velocities.

1 Introduction

The investigation of the shock properties of lightweight adobe [1] is mainly motivated by applications to impact [2, 3] and blast scenarios [4]. The goal is to conduct material tests from which a numerical model can be deduced that properly describes the shock loading of the material. Planar plate impact (PPI) experiments are an established technique [5] to gain information on the equation of state (EOS) properties, which mainly govern the reaction of a material to shock loading. PPI experiments have been performed on geological [6] as well as advanced concrete and masonry materials [7, 8]. For the inhomogeneous and low-strength lightweight adobe material, a corresponding investigation has been reported only very recently [1].

In Section 2, we summarize the experimental and numerical studies presented in Reference [1]. First, inverse PPI experiments with lightweight adobe specimens are described and the obtained free surface velocity time data is discussed. After that, the shock velocity vs. particle velocity relation obtained from this data is given. Then, the simplified representation of these PPI experiments in numerical simulations is introduced and the simulated free surface velocity time curves are compared to the experimental data. The adequate reproduction of the features in the experimental curves by the simulated ones allows us to conclude that the shock response of lightweight adobe is properly captured by the numerical model. In Section 3, this model is applied to an exemplary scenario of the ballistic impact of steel spheres on a lightweight adobe brick. In this example, a good reproduction of the experimental results is achieved by the numerical simulations. Consequently, this application demonstrates the predictive capabilities of the numerical model derived in Reference [1] towards ballistic impact in the given velocity range.

2 Shock response of lightweight adobe

In the following, we present a combined experimental and numerical approach to study the shock response of lightweight adobe. This combination allows overcoming the challenges in the evaluation and interpretation of the experimental data.

2.1 Planar plate impact experiments

The investigated lightweight adobe material is a commercial product (Claytec Leichtlehmstein 1200 NF). Its average density is 1.2 g/cm^3 and the quasi-static compressive cylinder strength was experimentally determined to be 2.8 MPa. Moreover, a longitudinal sound velocity of c_l = 656 m/s has been measured. Due to the content of chaff and pores (see top of Fig. 1), this material exhibits a significant degree of inhomogeneity.

From the purchased lightweight adobe bricks, specimens of cylindrical shape with a thickness of 8 mm and a diameter of approximately 50 mm have been manufactured. Since the surface of this material shows poor reflection of light, the PPI experiments are conducted in an inverse impact configuration (see Fig. 1). In this configuration, the point of measurement is situated on the well reflecting back surface of a witness

* Corresponding author: christoph.sauer@emi.fraunhofer.de

plate, which constitutes the target. This 2 mm thick C45 steel plate is impacted by a projectile consisting of a 2 mm thick C45 steel backing plate and the lightweight adobe specimen, attached to a guiding sabot.

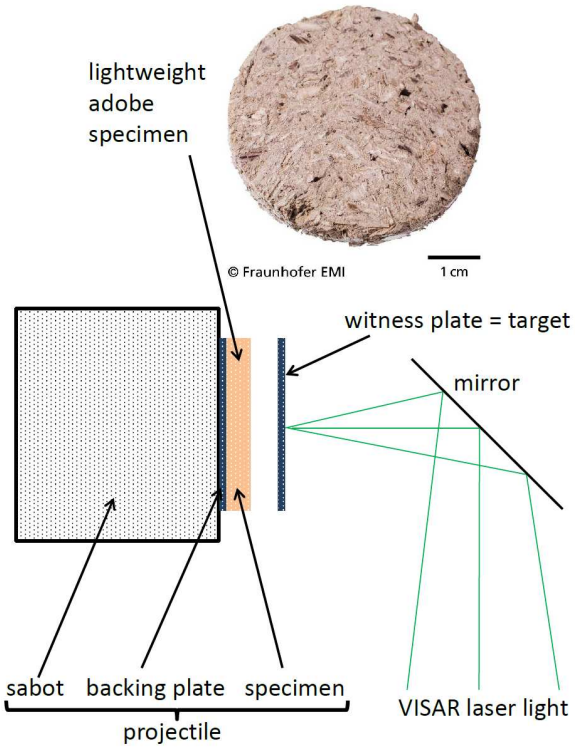

Fig. 1. Schematic depiction of the inverse planar plate experiment setup (bottom) together with a photograph of a lightweight adobe specimen (top).

The projectile is accelerated with a single-stage gas gun, which is operated with compressed air for impact velocities below 400 m/s and with gun propellant for higher impact velocities (up to 1000 m/s). Upon impact of the adobe specimen on the surface of the steel witness plate, shock waves are created, which travel through both materials. Depending on the specific wave propagation characteristics of the materials, the waves travel with certain velocities and are reflected and transmitted at the interfaces. Each wave reflection at the back surface of the witness plate leads to an acceleration of this surface and hence an increase of the free surface velocity. The change of this quantity with time is measured with a laser interferometer of the VISAR-type [9, 10, 11]. From these free surface velocity time curves, information of the initially produced shock state, release states, and general wave propagation characteristics of the specimen can be extracted. For a schematic illustration of the wave propagation in the inverse PPI experiment shown in Fig. 1 and its relation to the features in the free surface time velocity curves, we would like to refer the reader to Reference [1].

In Fig. 2, the free surface time velocity curves of the inverse PPI experiments with the lightweight adobe specimen for a series of different impact velocities are depicted. The most prominent feature in these curves is the steep increase before the final velocity, denoted as backing reflection in panels a) to c). It stems from the initial shock wave that has been reflected at the interface between specimen and backing plate. In panel d) this feature is also observable but becomes less distinct with decreasing impact velocity. Together with the general shape of the increase of the free surface velocity with time, the arrival time of the backing reflection carries information of the general wave propagation speed in the specimen. The height of the plateau after the first increase of the free surface velocity is related to the initial shock state, produced upon impact. It is called the 1st Hugoniot plateau. From this feature the shock data (shock velocity U_s vs. particle velocity u_p) of the specimen material can be gained, since shock response properties of the witness plate are known. The plateaus at higher free surface velocities are tied to release states and are thus denoted as release plateaus in Fig. 2a)-c). The fact that all these features, known from inverse PPI experiments of other porous materials [6, 7], can be identified in the data in Fig. 2, demonstrates that such a shock response investigation is feasible for lightweight adobe.

The identification of the 1st Hugoniot plateaus in the experimental curves displayed in Fig. 2 is based on the experience gained from the evaluation of other porous materials [6, 7]. First, the plateau of the curve from the experiment with the highest impact velocity is identified. Then the curve is averaged over a carefully chosen interval, resulting in the free surface velocity value of this 1st Hugoniot plateau. This is successively done for each curve with the next lower impact velocity. For the curves with the lowest impact velocities, the identified area of the 1st Hugoniot plateau is double checked by comparing the experimental curves with the corresponding curves of the numerical simulation. From the obtained velocity values, the shock velocities are calculated. For details on the identification of the 1st Hugoniot plateau and the calculation of the shock velocity and particle velocity see Reference [1].

From a linear fit ($U_s = c_B + S \cdot u_p$), we obtain a shock velocity – particle velocity relation of:

$$U_s = -10.1 \text{ m/s} + 2.04\, u_p \qquad (1)$$

with U_s and u_p in m/s. The data exhibits this linear relation in the particle velocity range from approximately 250 m/s to 900 m/s. However, the unphysical (negative) value of the bulk sound speed c_B shows that for smaller particle velocities the relation in Eq. (1) will not hold true. In this region a minimum of the shock velocity, similar to the situation in concrete [7, 12], is expected. This is due to the compaction of initially present pores in these materials.

2.2 Numerical modeling

The numerical simulations of the PPI experiments are performed with the commercial hydrocode software AUTODYN (Version 15.0). In such a hydrocode simulation the partial differential equations of the general conservation of mass, momentum, and energy are solved numerically together with a specific EOS and a particular constitutive model for each material [13].

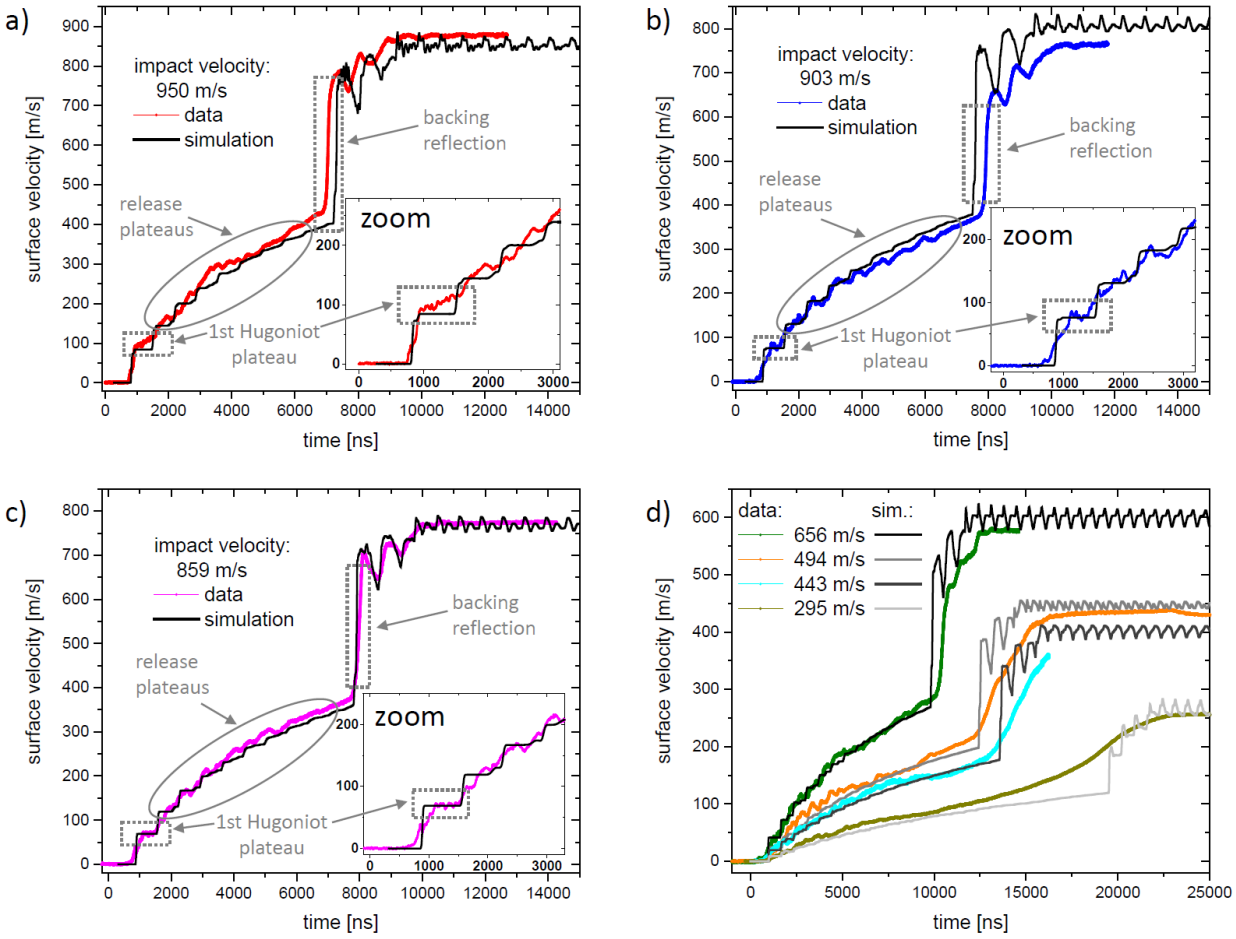

Fig. 2. Comparison of the simulated and measured free surface velocity time curves of inverse planar plate impact with lightweight adobe specimens and C45 steel backing and witness plates (see Fig. 1).

The geometry of the flyer plates (small thickness compared to diameter) leads to a state of uniaxial strain in the measurement area throughout the entire time of the measurement of the free surface velocity. This reduces the shock loading in these PPI experiments to a one-dimensional problem, which allows reproducing the experimental scenario in a simulation with a simplified geometrical setup. Explicitly, two-dimensional chains of elements are used for the projectile and the target. The motion of nodes into the direction perpendicular to the impact direction is hindered by a proper application of boundary conditions.

In these simulations, the C45 steel of the backing and witness plates is described by a shock EOS and a von Mises strength model. For lightweight adobe the RHT model [12] is used, as previously done and validated in References [2, 3] for an adobe material with a density of 1.8 g/cm^3. The central aspect of this model with respect to the shock loading in PPI is a p-α-EOS for the porous material and a polynomial formulation of the EOS of the fully compacted material. These take into account the pore compaction mechanism and its consequences for the relation of pressure, density, and internal energy.

The free surface velocity time curves obtained from the numerical simulations are presented in Fig. 2. For a direct comparison, each of them is superimposed with the corresponding experimental curve. The curve pairs in panels a) to c) are depicted separately, since a detailed comparison is performed for them. In Fig. 2a), the 1st Hugoniot plateau of the simulated curve is slightly lower than the one in the data. This appears to be the case for the release plateaus as well. In contrast, the height of all plateaus in panels b) and c) show a good agreement between simulated and measured curves. Furthermore, the backing reflection arrives slightly later in the simulated curve than in the corresponding measured curve in panel a). In panel b) the opposite is the case, while in panel c) both arrival times almost perfectly match. Moreover, the general shape of the increase with time of the measured free surface velocity is properly reproduced by the simulation for all curves in Fig. 2. Considering the significant degree of inhomogeneity in the lightweight adobe material, we can conclude that the numerical model manages to simultaneously reproduce all measured curves with reasonable accuracy. Hence, this homogenous numerical model is capable of a proper treatment of the shock response of the inhomogeneous lightweight adobe

material. Since the EOS properties play the central role in the material behavior under the shock loading that occurs in PPI, the employed porous p-α-EOS with the polynomial formulation of the solid EOS describe the shock response of lightweight adobe quantitatively correct.

3 Application to ballistic impact

In this section, the predictive capability of the previously introduced numerical model for lightweight adobe is tested. For that, we use an explicit example of a projectile impact. In the highly dynamic loading of such a scenario, the ballistic resistance of the target material is usually determined by both the constitutive model (i.e. strength and failure) and the EOS properties. Thus, both need to properly capture the corresponding behavior of lightweight adobe for a successful demonstration of predictive capabilities in such a scenario.

The numerical simulations are again performed with AUTODYN (Version 15.0). In this case a half-space 3D simulation of a spherical steel projectile impacting an upright standing lightweight adobe brick is performed. In the simulation and in the experiment the steel sphere has a diameter of 13.5 mm and the nominal dimensions of the lightweight adobe brick are 240 x 115 x 71 mm^3. Experiments are conducted analogous to the ones with targets consisting of a single adobe brick in References [2, 14]. Similarly, the hydrocode simulations are equal to the ones performed in Reference [2], but for the lightweight adobe target the material parameter set used in Subsection 2.2 and given in Reference [1] is employed.

In Fig. 3, a part of the results from these new experiments and simulations is presented. In the top part, an exemplary comparison of the simulated damage pattern with the penetration craters of the experiment is depicted. For the area of the simulated damage on the front side and the extent of experimental entrance crater a good agreement is found. For the analogous comparison of the rear side damage and the exit crater, target material seems to be missing from a slightly larger area than predicted by the simulated damage pattern. Turning to the residual velocities, illustrated in the bottom part of Fig. 3, an overall good agreement is found between experimentally determined and simulated values. For the lower impact velocities, the agreement is excellent. However, with increasing impact velocity there is a tendency for a growing deviation of the simulated values with respect to the measured ones towards smaller residual velocities. Additionally, the very small deformations of the spherical steel projectiles seen in the flash X-ray measurements behind the target are properly reproduced by the simulations for all impact velocities (X-ray vs. simulation not shown here). Thus, the full phenomenology of the ballistic impact experiments is properly reproduced by the simulations.

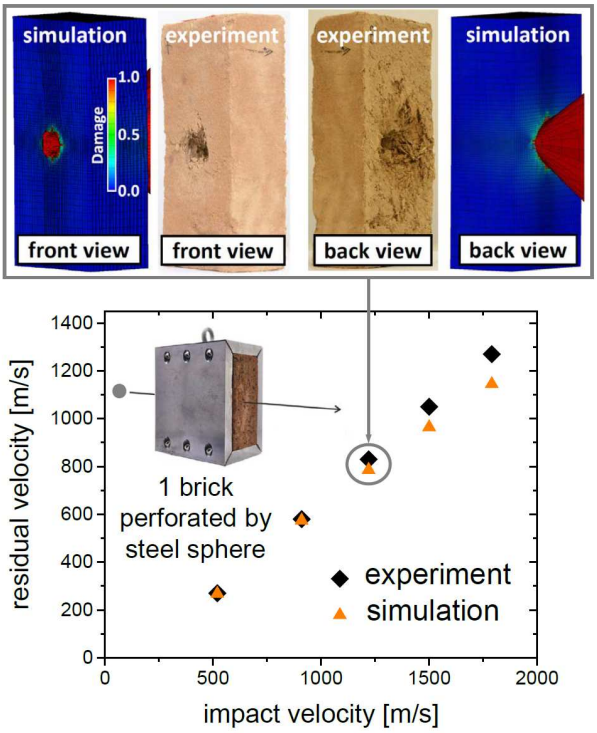

Fig. 3. Simulated and measured residual velocities of lightweight adobe targets perforated by steel spheres (bottom) together with an exemplary comparison of a simulated damage pattern with the experimental penetration craters (top).

4 Conclusion

This contribution presents the development of a numerical model for the shock response of lightweight adobe and its successful application to an exemplary ballistic impact scenario.

The model development in Section 2 is based on planar plate impact (PPI) experiments and reasonably accurate numerical simulations of the experimental curves by utilizing the established RHT-model [12] for the description of lightweight adobe. It is demonstrated that PPI experiments are feasible for such a low-strength, lightweight, and porous geological construction material and that a shock velocity vs. particle velocity relation can be determined from the measured free surface velocity time curves. For the latter, the combination of experiment and simulation is crucial. Details of the work summarized in Section 2 can be found in Reference [1]. In Section 3, this numerical model is applied to the impact of steel sphere projectiles on lightweight adobe brick targets. The results of these simulations show an adequate reproduction of the full phenomenology of the experiments.

Consequently, the applied homogenous numerical model properly describes the shock loading of the significantly inhomogeneous lightweight adobe in PPI and the penetration of spherical projectiles. Hence, for the presented scenarios, the underlying physics with respect to the equation of state, strength, and failure are simultaneously captured by this numerical model with quantitatively sufficient accuracy.

We acknowledge funding by BAAINBw and BMVg.

References

1. C. Sauer, F. Bagusat, A. Heine, W. Riedel, J. Dyn. Behav. Mater. (submitted)
2. C. Sauer, A. Heine, W. Riedel, Int. J. Impact Engng. **104**, 164-176 (2017)
3. C. Sauer, A. Heine, K. E. Weber, W. Riedel, Int. J. Impact Engng. **109**, 67-77 (2017)
4. C. Roller, C. Mayrhofer, W. Riedel, K. Thoma, Engng. Struc. **55**, 66-72 (2013)
5. M. A. Meyers, *Dynamic behavior of materials* (New York: John Wiley & Sons-Verlag, 1994)
6. T. Hoerth, F. Bagusat, S. Hiermaier, Int. J. Impact Engng. **90**, 122-130 (2017)
7. W. Riedel, M. Wicklein, K. Thoma, Int. J. Impact Engng. **35**, 155-171 (2008)
8. W. D. Reinhart, Proceedings of the 12th Hypervelocity Impact Symposium, Baltimore, MD, USA, 2012
9. L. M. Barker, R. E. Hollenbach, J. Appl. Phys. **43**, 4669-4675 (1972)
10. L. M. Barker, K. W. Schuler, J. Appl. Phys. **45**, 3692-3693 (1974)
11. W. F. Hemsing, Rev. Sci. Instrum. **50**, 73-78 (1979).
12. W. Riedel, N. Kawai, K. Kondo, Int. J. Impact Engng. **36**, 283-293 (2009)
13. J. A. Zukas, *Introduction to Hydrocodes*, Elsevier Ltd. 2004, First Edition, ISBN 0-08-044348-6
14. A. Heine, M. Wickert, Proceedings of the 29th International Symposium on Ballistics, Edinburgh, Scotland, UK (2016)